



## OPEN ACCESS

EDITED BY  
Alfredo Satyanaga,  
Nazarbayev University, Kazakhstan

REVIEWED BY  
Robby Yussac Tallar,  
Universitas Kristen Maranatha, Indonesia  
Eriko Dewangga,  
Nazarbayev University, Kazakhstan

\*CORRESPONDENCE  
Achmad Syarifudin,  
✉ [achmad.syarifudin@binadarma.ac.id](mailto:achmad.syarifudin@binadarma.ac.id)

RECEIVED 21 November 2025  
REVISED 29 November 2025  
ACCEPTED 30 November 2025  
PUBLISHED 01 April 2026

CITATION  
Muhsin, Maricar F, Lopa RT and  
Syarifudin A (2026) A flood protection  
model integrating gate operation,  
pumping system, and polder storage of  
Ogan Ilir watershed.  
*Front. Built Environ.* 11:1751381.  
doi: 10.3389/fbuil.2025.1751381

COPYRIGHT  
© 2026 Muhsin, Maricar, Lopa and  
Syarifudin. This is an open-access  
article distributed under the terms of  
the [Creative Commons Attribution  
License \(CC BY\)](https://creativecommons.org/licenses/by/4.0/). The use, distribution or  
reproduction in other forums is  
permitted, provided the original  
author(s) and the copyright owner(s) are  
credited and that the original  
publication in this journal is cited, in  
accordance with accepted academic  
practice. No use, distribution or  
reproduction is permitted which does  
not comply with these terms.

# A flood protection model integrating gate operation, pumping system, and polder storage of Ogan Ilir watershed

Muhsin<sup>1</sup>, Farouk Maricar<sup>1</sup>, Rita Tahir Lopa<sup>1</sup> and  
Achmad Syarifudin<sup>2\*</sup>

<sup>1</sup>Department of Civil Engineering, Hasanuddin University, Makassar, Indonesia, <sup>2</sup>Department of Civil Engineering, Bina Darma University, Palembang, Indonesia

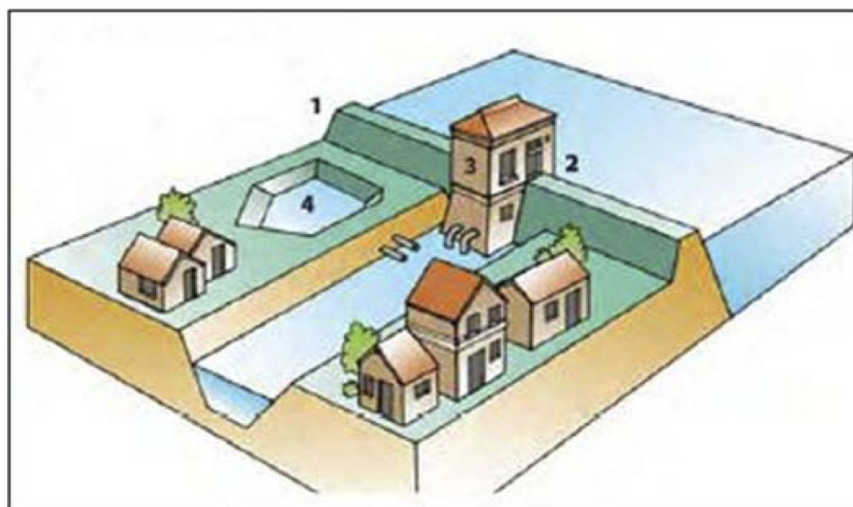
Flooding is a problem that causes losses, so efforts to solve flood problems are efforts to minimize losses. To reduce the losses caused as much as possible, there are several approaches to overcome losses through incident management and its impacts. The purpose of this study is to investigate variations in water levels in the Ogan Ilir Watershed in order to monitor fluctuations in water levels to prevent current and future flood problems. This study was conducted by analyzing the flow hydrodynamics in a channel with an area of 256,590 ha using the HEC-RAS program with rainfall data and flow hydraulics data. The results of the analysis showed that there was a very significant change in the inundation area that occurred amounting to an area of 256,490 ha and after the integration simulation between the construction of retention ponds, polders, and the operation of sluice gates simultaneously, there was a reduction in inundation of almost 60% of the watershed area or 153,894 ha.

## KEYWORDS

flap gate, flood, HEC-RAS, Ogan Ilir watershed, polder, retention pond

## 1 Introduction

Flooding is a disaster in Indonesia due to the overflow of river. In Ogan Ilir which located on South Sumatera is highly prone to flooding. Particularly influenced by the Ogan Ilir river and its tributaries. In Ogan Ilir, the dominance of lowland and there are so many shrubs indicate that areas are more prone to flooding. A polder system is a flood management system that utilizes comprehensive physical infrastructure, including drainage channels, retention ponds, and water pumps, all controlled as a single management unit. The polder system clearly demarcates flood-prone areas, allowing for control over water levels, discharge, and the volume of water released from the system. Therefore, the polder system is also known as a controlled drainage system. This system is used in low-lying areas and basins where water cannot flow by gravity. To prevent flooding, channels are constructed around the basins (Horváth et al., 2022; Hu et al., 2024). In the past three decades, Indonesia's rapid economic development and growing population have led to extensive conversions of agricultural land and land reclamation, primarily for industrial and urban development. Uncontrolled land use changes can render low-lying areas highly vulnerable to inundation. According to previous studies (Suryadi et al., 2014), when an area is developed for urban purposes and exceeds 60% of the total available area, it is considered prone to flooding. In general, a polder system consists of dikes, drains, retention ponds and outlet structures or pumping stations. An



Notation	Description
1	Closed dyke-ring
2	Dyke-ring surrounding the polder area
3	Pumping station, to discharge the rainfall and to control the water level inside the polder
4	Retention basin

FIGURE 1 Component of polder system (Witteveen+Bos, 2009; Suryadi et al., 2014).

integration of all components in one polder system can create one integrated polder system as shown in Figure 1 (Suryadi et al., 2014).

### 1.1 Ogan Ilir watershed

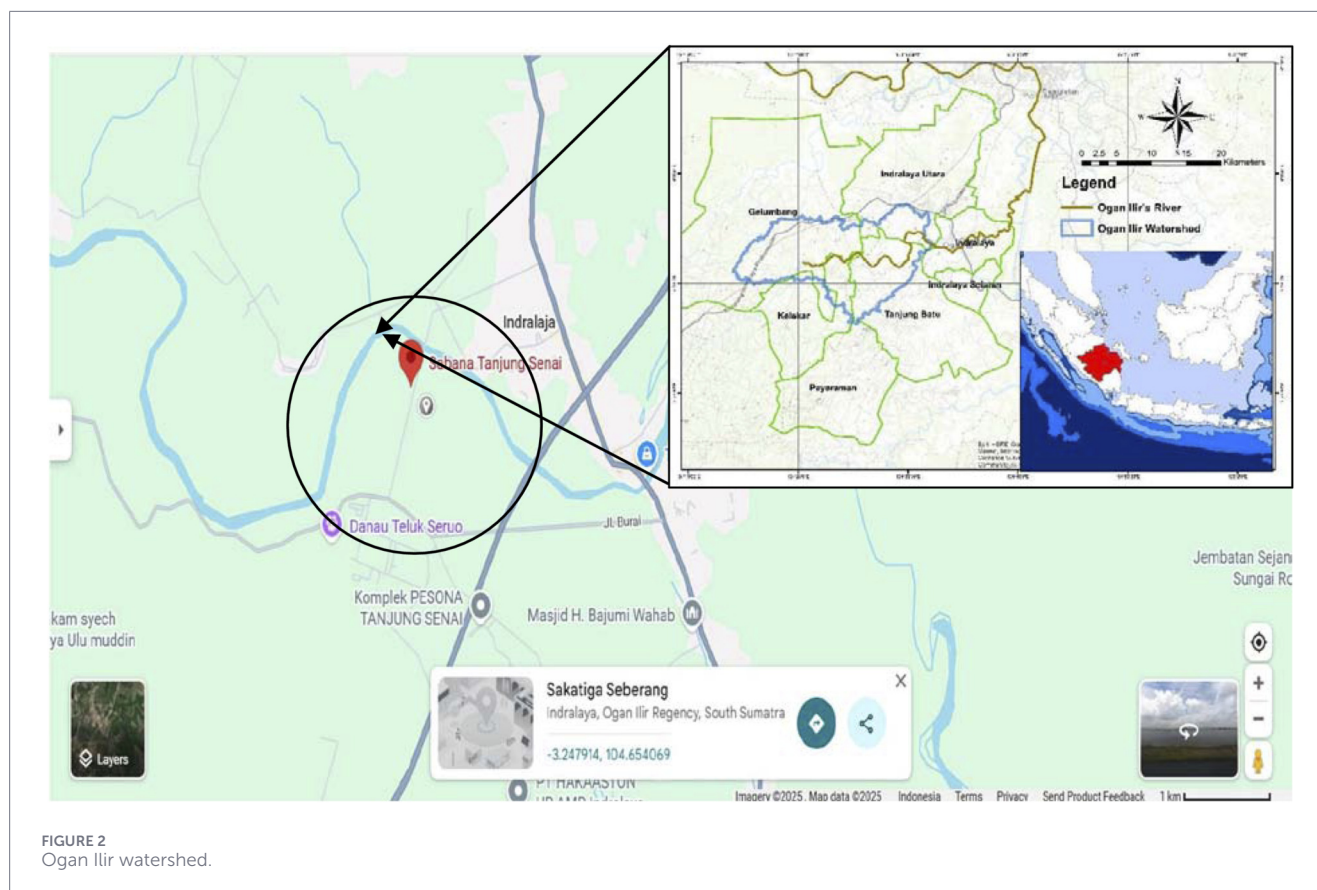
The Ogan Ilir Watershed in South Sumatra is indeed prone to flooding, especially during the rainy season. Flooding in the area has been reported on several occasions, including: 11 March 2024: Flooding occurred in Indralaya District and West Pemulutan District due to high-intensity rain, affecting villages such as Indralaya Mulya, Tanjung Seteko, and Kamal. The floodwaters gradually receded, but not before affecting 324 people. 31 January 2024: Flooding hit Pemulutan District, affecting 138 families and causing damage to 138 housing units, 2 educational facilities, and 1 worship facility. The floodwaters reached depths of 10–40 cm. May 2023: Flooding was reported in Ogan Ilir Regency, with details available on Relief Web (<https://adinet.ahacentre.org>).

These flooding incidents highlight the importance of effective water management and flood mitigation measures in the Ogan

Ilir Watershed. The watershed’s hydrological characteristics are influenced by its morphometric conditions, geomorphology, and climatology (Figure 2).

### 1.2 Polder system

The Polder system is defined as a closed system of water flow flowing with the help of a pump and the flow of water in the system can be monitored and regulated in and out of the closed system. In its application, a simple polder system has been applied since ancient times such as in China for irrigation purposes where the water flow system is closed and can be regulated as well as to protect the irrigation area inside from water from outside the system. In its development, the Polder system was used in the Netherlands to overcome the problem of flooding (Christian, 2022). The model of service index of polder systems is needed urgently in order to make the standard of polder’s condition criteria. This model should combine the technical aspects and non-technical aspects for prioritize polder maintenance, because both



aspects would support the water resources management in future. Technical aspects have connection with the function of polders, while organization, budgeting, economic, social and legal aspects as non-technical aspects could examine the polder services. Besides that, the stakeholder's participation and the community live in the polders (Noviadriana et al., 2025).

The Polder system itself is defined as a closed system of water flow flowing with the help of a pump and the flow of water in the system can be monitored and regulated in and out of the closed system. In its application, a simple polder system has been applied since ancient times such as in China for irrigation purposes where the water flow system is closed and can be regulated as well as to protect the irrigation area inside from water from outside the system (Noviadriana et al., 2025).

The use of polders in the Netherlands is caused by the sea level being higher than the land elevation of the Netherlands so that all wastewaters cannot be channeled into the sea and the influence of sea tides on the plains of the Netherlands. The existence of this problem makes Polder the solution (Christian, 2022; Ignatius et al., 2019).

A polder system is a flood management method that utilizes a complete set of physical infrastructure, including drainage channels, retention ponds, and water pumps, all controlled as a single management unit. A polder system clearly demarcates flood-prone areas, allowing for control of water levels, discharge, and the volume of water drained from the system. Therefore, a polder system is also known as a controlled drainage system. Theses system is used in low-lying areas and depressions where water cannot flow by gravity. To

prevent flooding, channels are constructed around the depression. Water captured in the depression is collected in a reservoir and then pumped to a holding pond (Ignatius et al., 2019).

A retention pond is a pool/reservoir that collects rainwater for a specific period of time. Its function is to reduce peak flooding in a body of water/river. A retention pond is a basin or pool that can hold or absorb water, depending on the type of wall and base lining material. It is naturally present and can be utilized either in its original state or through adjustments. Generally, the design of this type of pond combines its function as a water storage pond with use by the community and the surrounding environmental conditions. This type of natural pond, in addition to serving as a storage area, can also absorb water in pervious areas or ponds, such as soccer fields (covered with grass), natural lakes, such as those found in recreational parks, and swamp ponds (Ignatius et al., 2019).

## 2 Method and data

This survey was carried out after studying maps that were the result of the secondary data collection stages.

### 2.1 Method

The description of the methodology which is quite long can be seen briefly through the flow chart image of the implementation of this research, which is shown in the Figure 3. Research Flow Chart below.

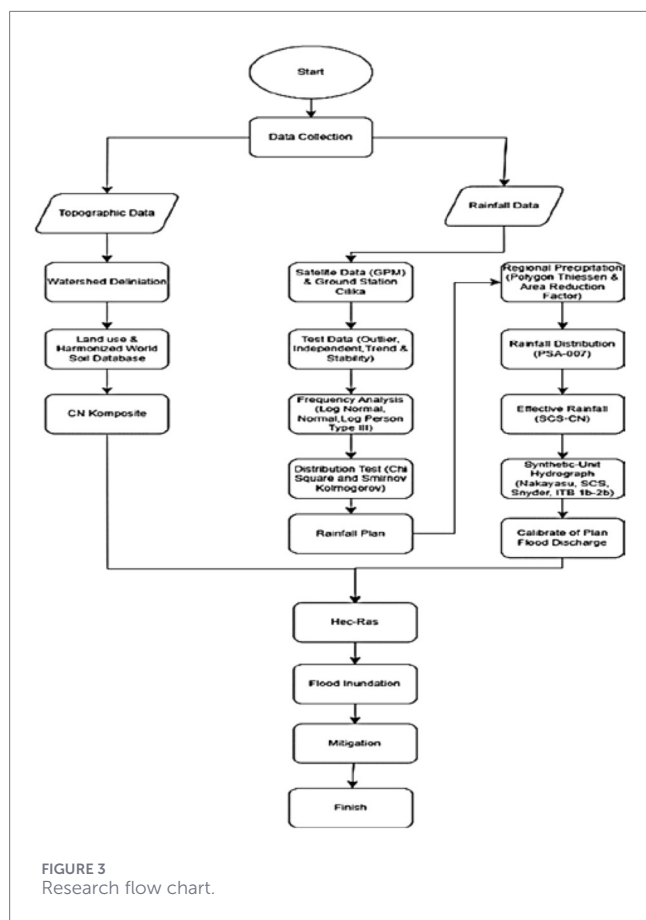


FIGURE 3 Research flow chart.

## 2.2 Hydrology and hydraulic analysis method

The land cover analysis represents the physical characteristics of the catchment, which are then used to determine the Curve Number (CN)—a hydrological parameter formulated by the Soil Conservation Service (SCS) to describe watershed response. Daily satellite rainfall data from 2001 to 2024 were utilized and subsequently adjusted using observations from the nearest rain gauge, UPTD Cilika, for corresponding years. The station data were first evaluated through several quality-control assessments, including outlier detection, independence testing, data stability, and trend acceptability.

Rainfall frequency analysis was carried out using log-normal, normal, log-Pearson type III, Gumbel, and exponential distributions (L-Moments), with the selected model required to satisfy both the Kolmogorov–Smirnov and Chi-Square goodness-of-fit tests. The design rainfall for a 100-year return period was then obtained. Spatial rainfall estimation employed the Thiessen polygon method combined with an Area Reduction Factor (ARF), while temporal distribution followed PSA 007 guidelines to derive effective rainfall using the SCS-CN procedure.

Flood design discharges were computed using several Synthetic Unit Hydrograph (SUH) approaches, including the SCS, Snyder, and ITB 1b–ITB 2b methods. Additional Synthetic Unit Hydrograph methods, including those proposed by Nakayasu and other approaches, were also applied. Calibration of the modelled flood

discharge was conducted using the bank full flow conditions as reference.

Flood simulations were performed using HEC-RAS ver. 6.6, with selected return-period rainfall inputs for validation purposes. The 20-year design flood was used as the primary scenario to meet regulatory requirements in accordance with the Ministers of Public Works Regulation No. 12/PRT/M/2014.

## 2.3 Data

The data collected from multiple sources and on-site observations were categorized into several key components, including rainfall, land-use information, topographic surveys, and documented flood events, all of which are essential for the subsequent analyses. Delineation of the watershed was carried out using the HEC-HMS software to enable a more detailed hydrological assessment. The watershed was further one basin, as illustrated in Figure 4 (BPS-Statistics Ogan Ilir regency, 2025).

### 2.3.1 Rainfall data

Given the limitations of available ground-based rainfall records, satellite observations were utilized as an alternative source of precipitation data. In this study, rainfall estimates were obtained from the Global Precipitation Measurement (GPM) product, which provides precipitation information suitable for hydrological analysis and spatial rainfall mapping. GPM offers a spatial resolution of  $0.1^\circ \times 0.1^\circ$  (approximately  $10 \text{ km} \times 10 \text{ km}$ ) and a temporal resolution of 30 min. The closest ground observation point is the Cilika rainfall station.

The Ogan Ilir River watershed intersects six GPM grid cells, and the centroid of each cell was used as the reference point for extracting daily satellite precipitation values. The distance between each grid and the Cilika station was further incorporated as a correction variable to enhance the accuracy of satellite-derived rainfall. The station’s rainfall observations are shown in Figure 4 (NASA, 2025).

Daily GPM data from all grids were then adjusted based on ground observations using a monthly selection approach. When a monthly correlation coefficient exceeded 0.6 but the RMSE remained unacceptable, daily rainfall data were not directly comparable to the monthly series. This mismatch is often caused by temporal displacement of GPM rainfall peaks relative to ground measurements—typically shifting forward or backward by several days. For this reason, the relationship between satellite and station data was evaluated using probability-based comparison rather than direct time-series alignment. The resulting GPM ratio values are presented in Table 1, while the correction trendline is illustrated in Figure 5 (NASA, 2025).

Validation of the GPM dataset against ground observations indicates a strong correlation within the study basin, particularly consistent with equatorial rainfall characteristics, and yields an RMSE of 0.735%. A correction factor was subsequently derived and applied to adjust the GPM data. The corrected rainfall series, obtained by applying the calibration equation to the raw GPM values, is shown in the following figure (NASA, 2025).

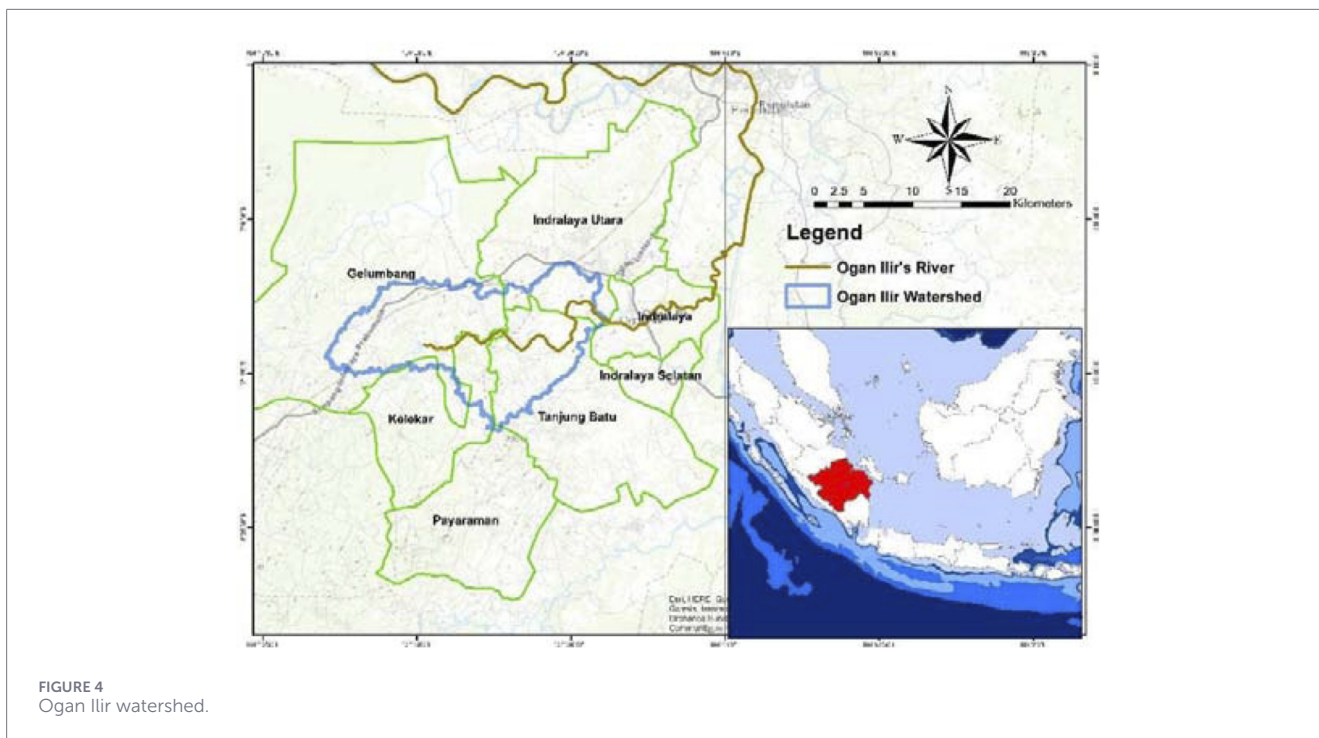


FIGURE 4  
Ogan Ilir watershed.

TABLE 1 GPM ratio.

Min	Rainfall station	GPM	Ratio	Multiplier	Enhancer
Class 1	8.11	13.60	0.60	0.31	-3.65
Class 2	12.00	15.52	0.77	0.09	-0.66
Class 3	16.10	18.43	0.87	0.03	0.24
Class 4	20.40	21.68	0.94	0.02	0.49
Class 5	25.49	26.51	0.96	0.00	0.85
Class 6	33.00	31.71	1.04	0.02	0.56
Class 7	46.00	40.95	1.12	0.01	0.76
Class 8	120.30	81.01	1.49	0.01	0.75

### 2.3.2 Land-use and land cover

Land-use dynamics occurring across the region represent a critical factor influencing flood generation. In hydrological assessment, land cover and soil type are two fundamental components controlling the interaction between rainfall and the land surface. Land cover regulates interception, evapotranspiration, and surface roughness, while soil type determines the soil's infiltration capacity, permeability, porosity, and the rate at which water can be absorbed. These characteristics are central to the classification of Hydrologic Soil Groups (HSG)—ranging from A (highly permeable) to D (very low permeability) which are used in assigning Curve Number (CN) values. Areas dominated by sandy or well-drained soils (HSG A–B) typically exhibit high infiltration and low CN values, whereas clayey or compacted soils (HSG C–D) produce more direct runoff due to their limited capacity to store water. Thus, the distribution of soil types contributes significantly to the watershed's hydrological response, particularly under conditions of land-use change.

Land-cover data for the study were sourced from the Esri Sentinel-2 Land Cover dataset for 2023 reflected in [Figures 6A,B](#). The combined influence of altered land cover and the underlying soil characteristics has modified the Curve Number values for each sub-catchment within the Ogan Ilir watershed.

### 2.4 Hydrograph stream flow analysis

Frequency analysis is used to estimate rainfall by looking at the frequently used distributions ([Syarifudin, 2018](#)). Estimated rainfall plans are implemented using frequency analysis of annual maximum rainfall data (annual series). There are several statistics in the distribution, and four categories are frequently used in frequency analysis ([Syarifudin, 2018](#)) namely: 1. Log Normal 2-parameter; 2. Normal; 3. Gumbel Type I; 4. Log-Pearson Type III. Each distribution has different statistical properties. The suitable distribution for a given data set can be determined by calculating the statistical parameters of the investigated data set. The following are the intended statistical parameters: Statistical

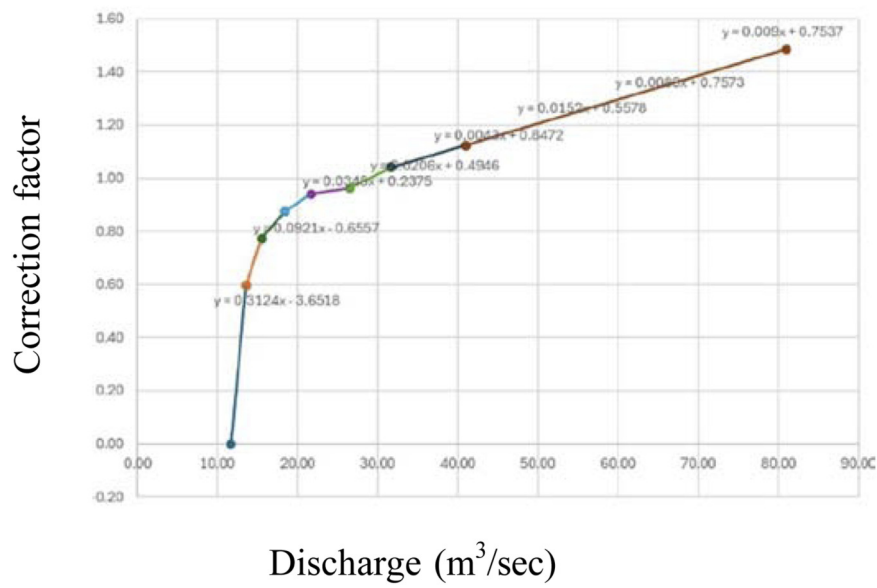


FIGURE 5  
Rainfall data correction trendline.

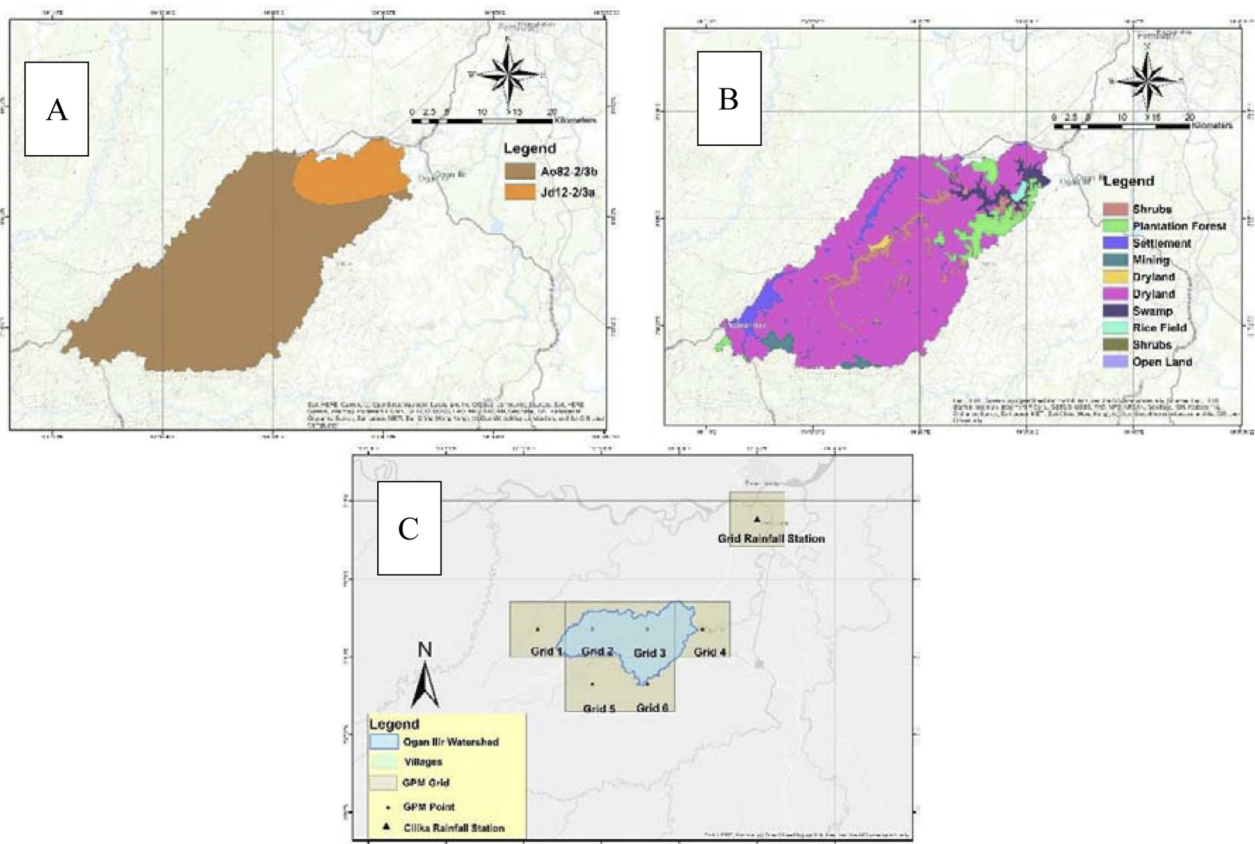


FIGURE 6  
(A) Land cover (B) land use (C) point of giovanni precipitation model.

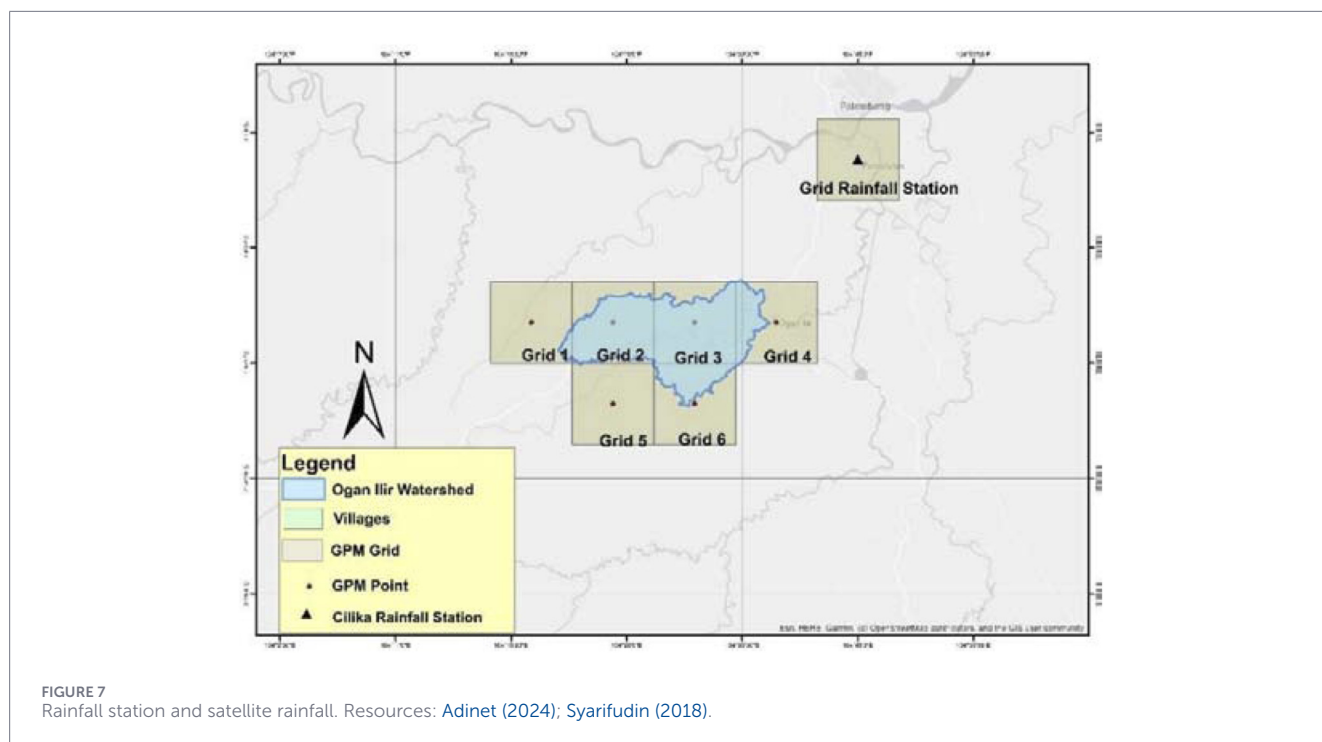


FIGURE 7  
Rainfall station and satellite rainfall. Resources: Adinet (2024); Syarifudin (2018).

TABLE 2 Rainfall correction.

Rainfall interval (mm)	Correction equation	Correction factor
GPM > 120.3	0.009029 + 0.753687	1.49
46 < GPM < 120.3	0.008939709 + 0.757349	1.12
33 < GPM < 46	0.015232634 + 0.557823	1.04
25.49 < GPM < 33	0.004316077 + 0.847196	0.96
20.4 < GPM < 25.49	0.020576289 + 0.494609	0.94
16.1 < GPM < 20.4	0.034527864 + 0.237534	0.87
12 < GPM < 16.1	0.09209342 - 0.655739	0.77
8.11 < GPM < 12	0.312443462 - 3.651839	0.6
GPM < 8.11	0	0

parameters commonly used to determine the suitable distribution include: Coefficient of skewness - Coefficient of kurtosis - Standard deviation - Mean (Syarifudin, 2018).

The Equations 2.1–2.5 are used such as below:

$$X = \frac{\sum xi}{n} \tag{2.1}$$

$$S = \sqrt{\frac{\sum (xi - xr)^2}{(n - 1)}} \tag{2.2}$$

$$Cs = \frac{n}{(n - 1)(n - 2)S^3} \sum (xi - xr)^3 \tag{2.3}$$

$$Ck = \frac{n}{(n - 1)(n - 2)S^4} \sum (xi - xr)^4 \tag{2.4}$$

$$Cv = \frac{S}{x} \tag{2.5}$$

with:

- X = Average value (mean value)
- S = Standard deviation
- Cs = “Skewness” coefficient (Skewness coefficient)
- Ck = kurtosis coefficient (kurtosis coefficient)
- Xi = rain data
- n = Mount of data

### 3 Results and discussion

#### 3.1 Hydrological analysis

To improve the accuracy of satellite-derived rainfall data in the Ogan Ilir Watershed, researchers are using Global Precipitation Measurement (GPM) data with a spatial resolution of 0.1°

TABLE 3 Rainfall distribution.

Distribution	XSquare			SmirnovKolmogorov		DMax
	a = 5%	Attained a	Arson para	a = 5%	Attained a	
Normal	ACCEPT	56.37%	0.33333	ACCEPT	98.76%	0.08111
Normal (L-Moments)	ACCEPT	56.37%	0.33333	ACCEPT	98.42%	0.08317
LogNormal	ACCEPT	56.37%	0.33333	ACCEPT	99.97%	0.06127
Galton				ACCEPT	99.94%	0.06375
Exponential	REJECT	3.74%	4.33333	ACCEPT	61.27%	0.14423
Exponential (L-Moments)	ACCEPT	6.79%	3.33333	ACCEPT	41.19%	0.1703
Gamma	ACCEPT	0.563703	0.33333	ACCEPT	0.99948	0.06297
Pearson III				ACCEPT	99.93%	0.06391
LogPearson III				ACCEPT	99.97%	0.0608
EV1-Max (Gumbel)	ACCEPT	56.37%	0.33333	ACCEPT	96.75%	0.09028
EV2-Max	ACCEPT	31.73%	1	ACCEPT	76.68%	0.12533
EV1-Min (Gumbel)	ACCEPT	31.73%	1	ACCEPT	63.84%	0.14112
EV3-Min (Weibull)	ACCEPT	31.73%	1	ACCEPT	83.90%	0.11562
GEV-Max				ACCEPT	99.95%	0.06247
GEV-Min				ACCEPT	99.81%	0.06892
Pareto				ACCEPT	91.27%	0.10364
GEV-Max (L-Moments)				ACCEPT	99.88%	0.06667
GEV-Min (L-Moments)				ACCEPT	99.73%	0.07079
EV1-Max (Gumbel, L-Moments)	ACCEPT	56.37%	0.33333	ACCEPT	95.49%	0.09413
EV2-Max (L-Moments)	ACCEPT	41.42%	0.66667	ACCEPT	80.71%	0.12006
EV1-Min (Gumbel, L-Moments)	ACCEPT	12.66%	2.33333	ACCEPT	58.00%	0.14823
EV3-Min (Weibull, L-Moments)	ACCEPT	31.73%	1	ACCEPT	81.94%	0.11838
Pareto (L-Moments)				ACCEPT	92.49%	0.10123
GEV-Max (kappa specified)	ACCEPT	31.73%	1	ACCEPT	60.29%	0.14543
GEV-Min (kappa specified)	ACCEPT	31.73%	1	ACCEPT	86.43%	0.11186
GEV-Max (kappa specified, L-Moments)	ACCEPT	19.67%	1.66667	ACCEPT	75.44%	0.12691
GEV-Min (kappa specified, L-Moments)	ACCEPT	31.73%	1	ACCEPT	84.69%	0.11447

TABLE 4 Rainfall distribution.

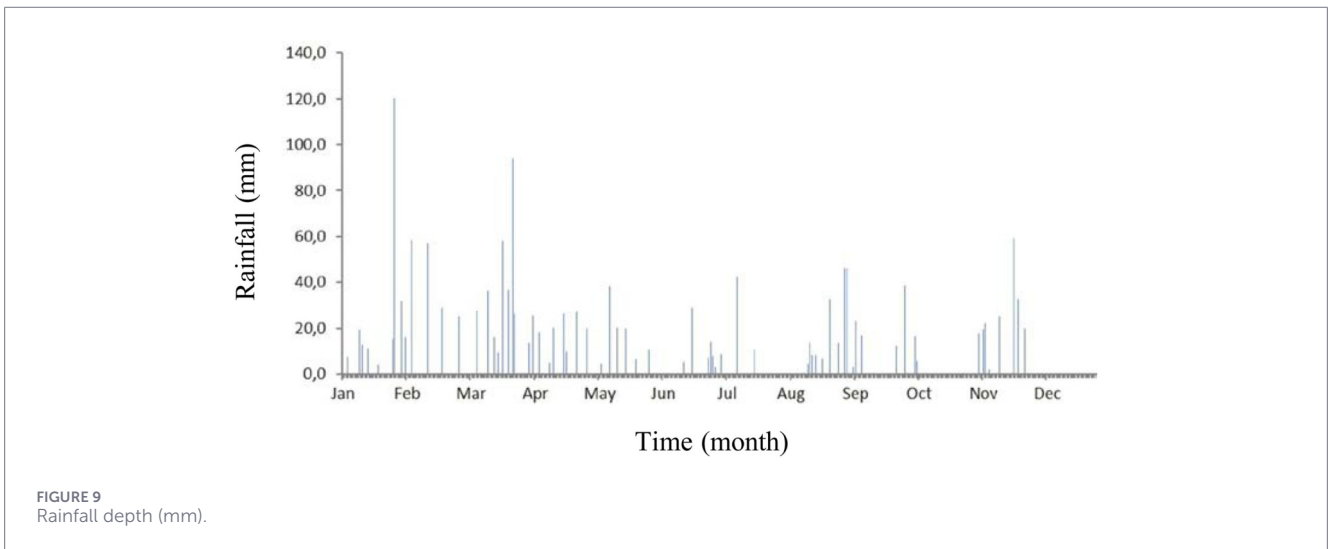
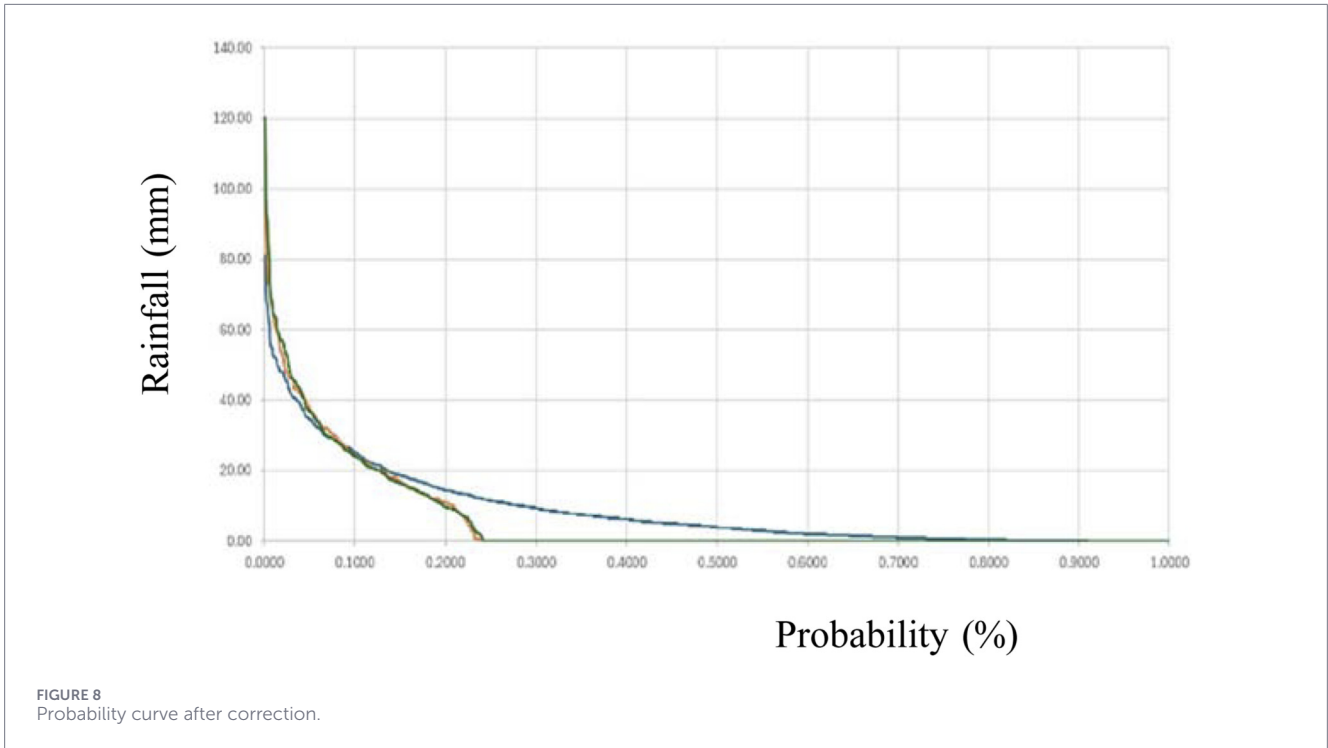
1. River name	Kelekar	
2. Watershed area (A)	256.590	km <sup>2</sup>
3. River lenght (L)	44.167	km
4. Rain height unit (R)	1.000	mm
5. Rain duration rate (Tr)	1.000	Jam
6. Effective rainfall	52.467	mm

× 0.1° (approximately 10 km × 10 km) and a 30-min temporal resolution. Here’s a breakdown of the process (Researchgate, 2010; Latif et al., 2019; Mustamin et al., 2021):

- Data Collection: GPM data is collected and divided into six grid sections, with each grid’s center point serving

as a reference coordinate for extracting daily satellite rainfall data.

- Correction Factor: The distance from the Cilika rainfall station is used as a correction factor to improve the accuracy of satellite-derived rainfall data. A correlation coefficient of 0.6 or greater is required for correction.
- Data Analysis: The correlation coefficient between GPM rainfall station and Cilika rainfall station is calculated, with a value of 0.8 indicating that rainfall correction with a correction factor can be applied.
- Probability Curve: The correction involves creating a probability curve of monthly maximum rainfall events within specific intervals. Calculations are based on monthly maximum rainfall data from 2011 to 2017.
- Correction Equations: The equations and correction factors for each interval are determined, and probability



curve graphs are created before and after the correction process.

Figure 7 shows that the consequences triggered by high intensity rain Monday 11 March 2024 at 17.00 WIB where the affected locations are Indralaya District; Indralaya Mulya Village; Tanjung Seteko Village; Opposite Sakatiga Village; West Pemulutan District; Kamal Village; State Island Village. To efforts: Carry out coordination with the local village government for further handling Latest Condition and the flood is gradually receding (Adinet, 2024).

Table 2 shows that the maximum rainfall correction factor for rainfall above 120 mm is 1.49. This indicates that the rainfall used is still within the tolerance limits for analysis the rainfall data in the study area (Aryastana et al., 2025; Syarifudin et al., 2022).

Figure 8 below shows the probability curve after correction, comparing rainfall depth with the percentage probability of occurrence (Aryastana et al., 2025).

### 3.2 Rainfall distribution

The results of the rainfall distribution analysis based on various distribution methods: normal, log-normal, log-Pearson Type 3, and Gumbel are shown in Table 3 below.

Based on the results of the analysis of the rainfall distribution method, the Log Normal method was chosen as it is suitable for the distribution of rainfall values recorded over the 15 years.

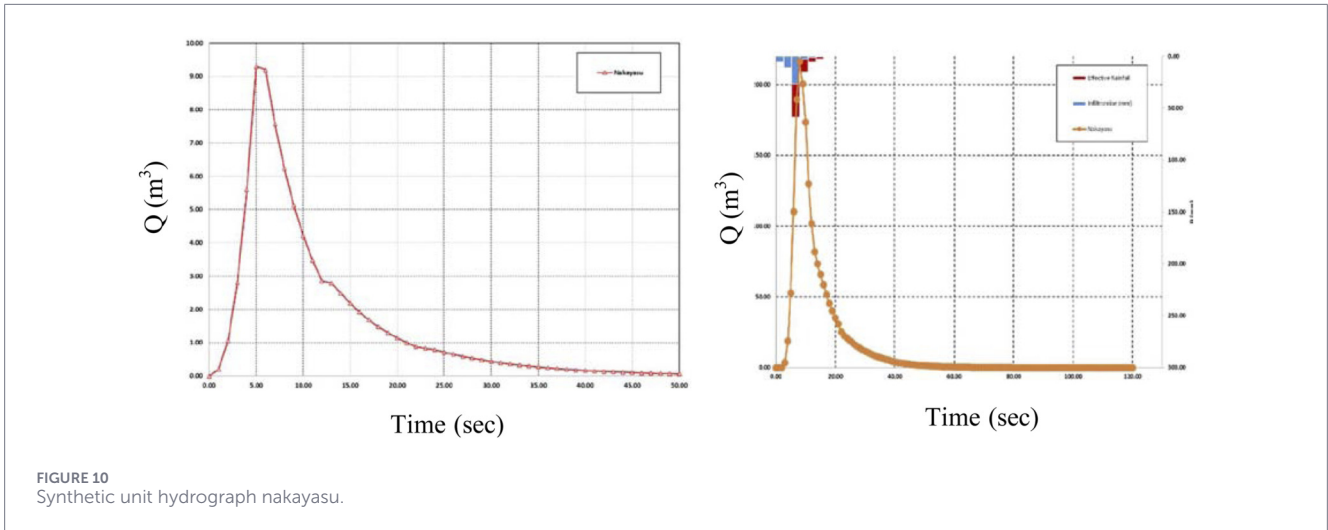


FIGURE 10 Synthetic unit hydrograph nakayasu.

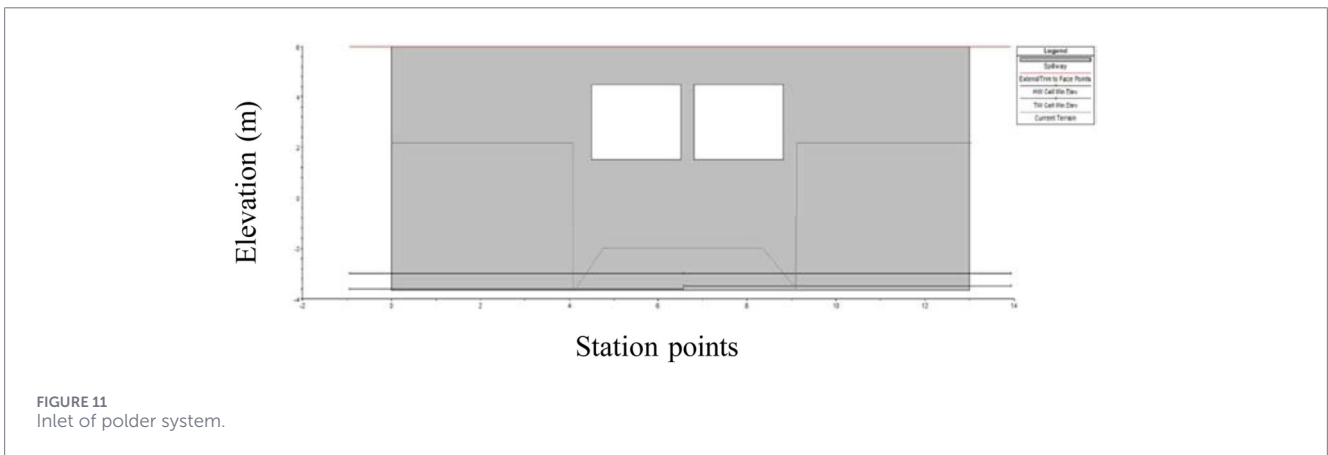


FIGURE 11 Inlet of polder system.

### 3.3 Regional rainfall analysis

Regional rainfall planning within a watershed is essential. If the analysis is only at the rainfall estimation post level, it is not yet the end of the watershed rainfall analysis. To determine the planned rainfall in a region, very long daily rainfall data is generally used. However, data availability in Indonesia is still very concerning, with the most widely available data being the maximum daily rainfall. To calculate the planned rainfall amount in a watershed using the annual maximum daily rainfall data as Equation 3.1. follows (NASA, 2025; Reliefweb, 2023):

$$P_{\text{basin}} = \text{ARF} \times P_{\text{max}} \tag{3.1}$$

The  $P_{\text{max}}$  value was calculated using the GEV frequency distribution with the help of the SMADA program. The  $P_{\text{max}}$  results can be seen in Table 4, while the ARF value can be determined. To find the maximum daily rainfall in the region, use daily rainfall data (NASA, 2025; Reliefweb, 2023).

The results obtained from the analysis of rainfall distribution are as shown in Figure 9.

The form of the synthetic unit hydrograph can be described as follows, as in Figure 10.

### 3.4 Inlet and pumping systems

Figure 11 shows the inlet of polder system where If a pump station is installed at a point in the river to control the height of the water level that will enter the pond (Satriani et al., 2021; Volker, 1983).

The flow system that enters the polder can be presented as in Figure 12 where there is a retention pond and there is a channel with sluice gates and culverts which function in stages to overcome standing water and overflow from the Kelekar River (Kalmah and Schultz, 2015; Ignatius et al., 2019).

During peak rainfall events, water levels within the drainage network can rise beyond the capacity of gravity-driven outflow. In tidal-influenced catchments, such as coastal or estuarine areas, high tide can block natural discharge, causing water to accumulate upstream. Pump-based mitigation provides an active mechanism to transport water across a hydraulic barrier by supplying sufficient head and discharge (Aryastana et al., 2025; NASA, 2025; Reliefweb, 2023).

Pumping systems are designed to:

1. Reduce water levels within inundated areas.

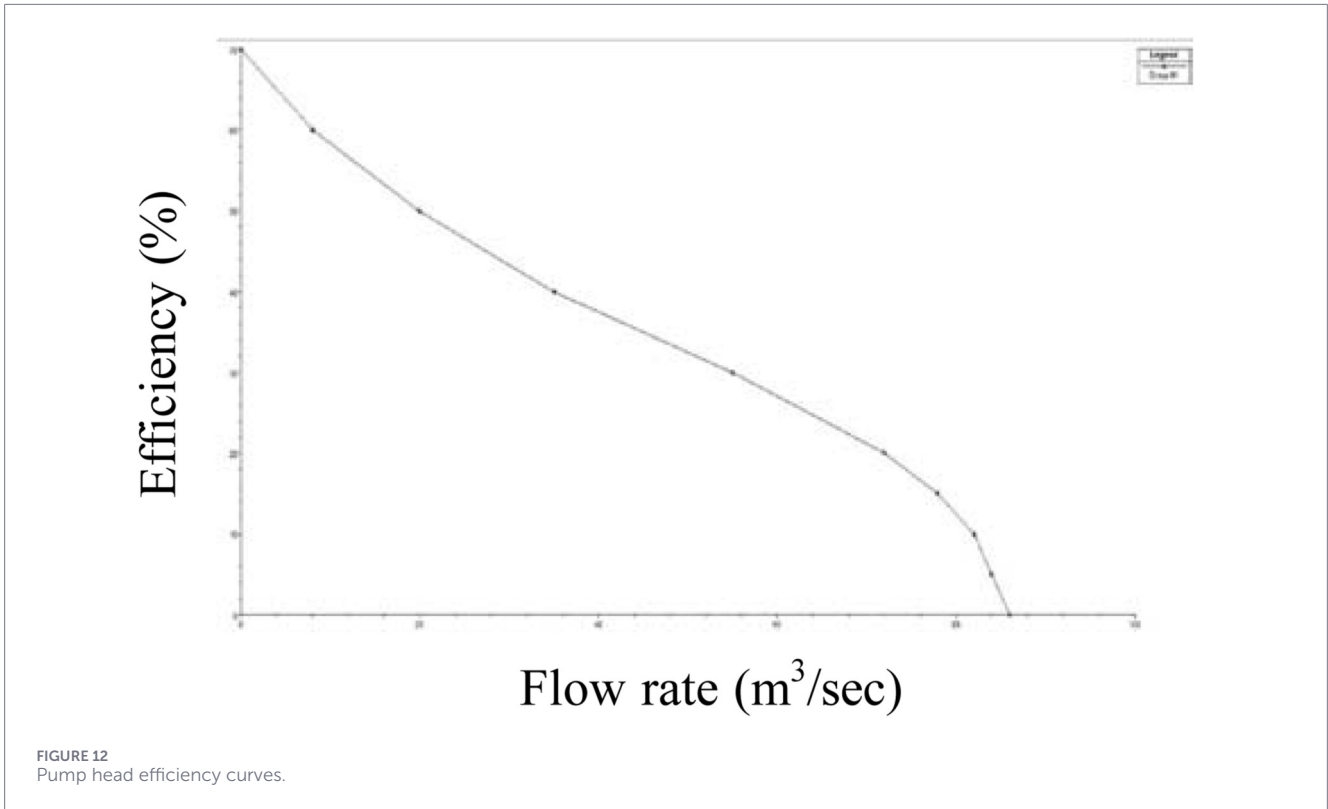


TABLE 5 Pump efficiency curves.

Head (m)	Flow (m <sup>3</sup> /s)
70	0
60	8
50	20
40	35
30	55
20	72
15	78
10	82
5	84
0	86

- Prevent prolonged ponding where drainage gradients are insufficient.
- Maintain discharge continuity during high-tide conditions.
- Shorten flood duration by rapidly removing accumulated water.
- Provide redundancy when structural drainage components (culverts, channels, gates) are insufficient.

The hydraulic performance of a pump is strongly influenced by the required Total Dynamic Head (TDH), the magnitude of inflow entering the inundated area, and the operational constraints of the receiving water body. Therefore, a detailed

hydrodynamic evaluation is essential to design an adequate pumping system.

After analyzing where the retention pond was pumped, the results showed a graph of high water efficiency when waterlogging occurred in the study area.

Flood mitigation in the study area also considers the use of pumping systems as an alternative structural measure to reduce inundation, particularly in low-lying zones where gravity drainage becomes ineffective during peak water levels or tidal backwater conditions. Pumping stations serve to actively remove excess water from the flooded area and discharge it into nearby channels or retention ponds, thereby reducing water depth and shortening inundation duration. The effectiveness of a pump system depends on several factors, including pump capacity, head requirements, operational efficiency, and the availability of a reliable power source. In tidal-affected regions such as the downstream section of the Pemaluan watershed, pumps play a crucial role during high-tide periods when natural outflow is obstructed. Therefore, a flood pump is often integrated with gates, culverts, and temporary storage basins to optimize water evacuation. Incorporating pump-based mitigation into the hydraulic model allows for assessing reductions in peak water level, identifying critical locations for pump installation, and determining the required pumping capacity to meet flood protection standards (Aryastana et al., 2025; NASA, 2025; Reliefweb, 2023).

The total head that must be overcome by the pump (H) is defined as the Equation 3.2:

$$H = H_{\text{static}} + H_{\text{tailwater}} + H_{\text{friction}} + H_{\text{minor}} \quad (3.2)$$

where:

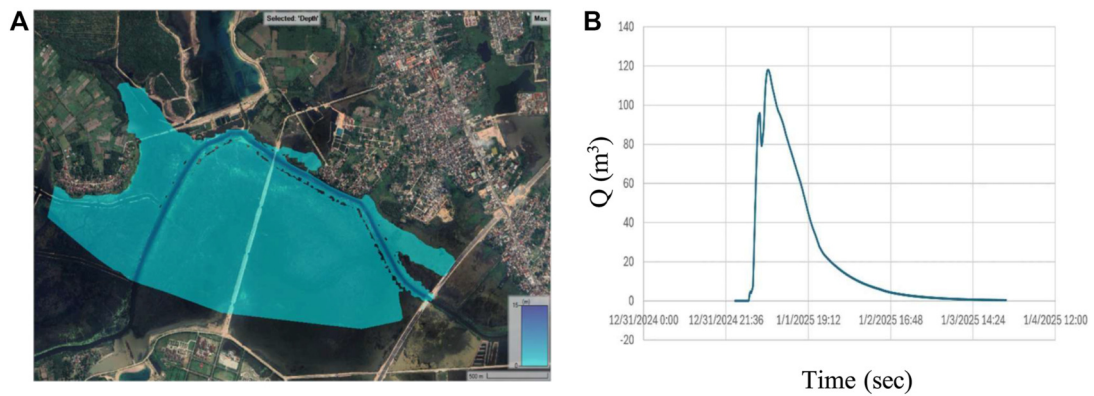


FIGURE 13 (A) Existing condition of Ogan Ilir basin (B) flow hydrograph.

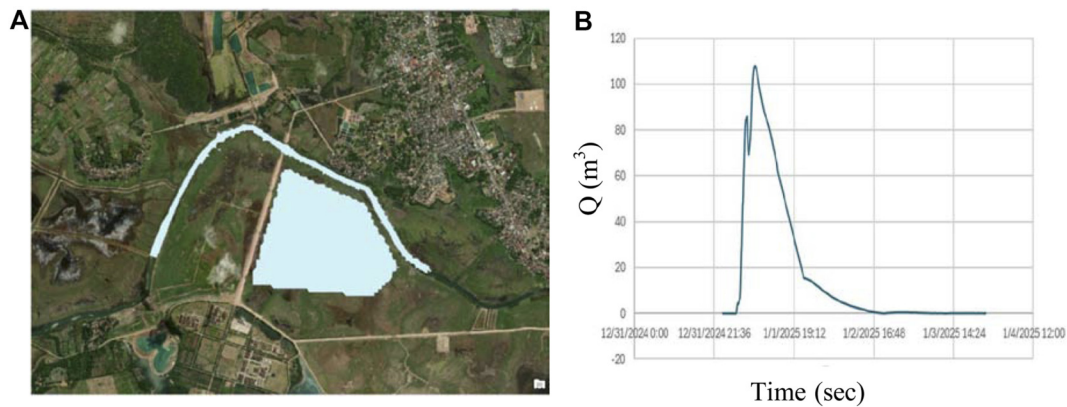


FIGURE 14 (A) Simulation result combine with retention pond, polder and gate. (B) Flow Hydrograph After Mitigation with Pond, Pump and Retention Polder.

- A. Static Head ( $H_{static}$ ): Static head corresponds to the vertical difference between the water level at the pump intake (sump) and the water level at the discharge outlet. In flood conditions, this value may vary depending on the depth of inundation.
- B. Tailwater Head ( $H_{tailwater}$ ): Tailwater head accounts for the influence of the receiving water body. In tidal zones, the pump must discharge against the highest predicted water level, making the design highly sensitive to tidal elevation and frequency.
- C. Friction Losses ( $H_{friction}$ ): Friction losses occur due to resistance between water and the inner pipe wall. These losses depend on pipe length, diameter, flow velocity, and roughness. They are calculated using the Darcy–Weisbach Equation 3.3:

$$hf = f \cdot \frac{L}{D} \cdot \frac{v^2}{2g} \tag{3.3}$$

To achieve reliable hydraulic estimation, friction losses are computed using the Darcy–Weisbach. The friction factor may be estimated using the Moody chart or the Colebrook–White equation, depending on Reynolds number and pipe roughness as Equation 3.4:

- D. Minor Losses ( $H_{minor}$ ): Minor losses include head reductions caused by bends, valves, inlets, outlets, and transitions. These are included via loss coefficients of Equation 3.4:

$$H_{minor} = K_{total} \cdot \frac{v^2}{2g} \tag{3.4}$$

where  $K_{total}$  is the sum of all individual loss coefficient.

Table 5 shows the head height value in relation to the flow rate that occurs due to pump efficiency (Hu et al., 2024).

### 3.5 Combination retention pond, pump and polder

#### 3.5.1 Existing condition

The following image shows the conditions at the study location, showing the extent of the flooding that occurred (Figure 13). The flood discharge that occurs in existing conditions with  $Q_{20}$  is  $117 \text{ m}^3/\text{s}$  in Figure 13A and the flow hydrograph in Figure 13B.

### 3.5.2 Analysis after mitigation with retention pond and pump

After that, a simulation was carried out with a combination of flow capacity limits with  $Q_{20}$  discharge as shown in the Figure 14.

The flood discharge that occurs in existing conditions with  $Q_{20}$  is  $102 \text{ m}^3/\text{s}$  in Figure 14A and the flow hydrograph in Figure 14B.

The integrated simulation demonstrates the effectiveness of combining retention ponds, polders, and sluice gate operations in reducing inundation (Sumi et al., 2013; Stowa/MX Systems, 2002; Salam et al., 2014).

- 60% reduction in inundation area: Approximately 153,894 ha of the watershed area would no longer be inundated.
- Initial inundation area: 256,490 ha.
- Final inundation area: 102,596 ha after implementing the integrated simulation.

This approach can help mitigate flooding and its associated impacts on communities and ecosystems. The peak flood discharge ( $Q_p$ ) that occurred was reduced by  $102 \text{ m}^3/\text{s}$ , there was a significant reduction in inundation of 85% with combined mitigation of retention ponds, polders, pumps and valve gate operations.

## 4 Conclusion

From this research, the following can be concluded:

1. A maximum rainfall occurred in February with a depth of 120 mm, then decreased in March to 90 mm. Rainfall continued to decrease in the following months and increased again in December to 60 mm. Peak discharge was calculated using the Nakayasu Synthetic Hydrograph method at  $9.3 \text{ m}^3/\text{s}$ .
2. The analysis shows that water efficiency is higher when inundation occurs in the study area after the construction of retention ponds. The analysis results show a very significant change in the inundation area.
3. An integrated simulation of the construction of retention ponds, polders, and sluice gate operations simultaneously shows a reduction in inundation of almost 60% of the watershed area, or approximately 153,894 ha. Initial inundation area of 256,490 ha can be reduced to 102,596 ha after the implementation of the integrated simulation.

Recommendations from the conclusions:

1. Increasing Retention Pond Capacity: Based on simulation results, the construction of retention ponds has shown significant results in reducing flooding. Therefore, increasing retention pond capacity should be considered to improve flood control efficiency.
2. Optimal Floodgate Operation: Optimal floodgate operation is crucial for controlling flooding. Therefore, further analysis

is needed to determine the optimal floodgate operation schedule.

3. Infrastructure Maintenance and Care: Flood control infrastructure, such as retention ponds and floodgates, requires regular maintenance and care to ensure optimal function.
4. Community Education and Training: The community needs to be educated and trained on the importance of flood control and how to reduce flood risk.
5. Development of Early Warning Systems (EWS): Developing early flood warning systems can help communities anticipate and reduce flood risk.
6. Integration with Spatial Planning: Flood control needs to be integrated with spatial planning to ensure that development does not increase flood risk.

## Data availability statement

The original contributions presented in the study are included in the article/supplementary material, further inquiries can be directed to the corresponding author.

## Ethics statement

The studies involving humans were approved by Prof. Rita, head of doctoral study program of Universitas Hasanuddin, Makassar, Indonesia. The studies were conducted in accordance with the local legislation and institutional requirements. The participants provided their written informed consent to participate in this study. Written informed consent was obtained from the individual(s) for the publication of any potentially identifiable images or data included in this article.

## Author contributions

Muhsin: Writing – review and editing, Investigation, Data curation, Formal Analysis. FM: Formal Analysis, Supervision, Methodology, Writing – review and editing, Validation, Conceptualization. RL: Formal Analysis, Methodology, Validation, Supervision, Writing – review and editing, Conceptualization. AS: Formal Analysis, Writing – original draft, Conceptualization, Methodology, Writing – review and editing.

## Funding

The author(s) declared that financial support was not received for this work and/or its publication.

## Acknowledgements

The authors acknowledge the contributions of Regent of Ogan Ilir Regency who provided valuable support in the research.

## Conflict of interest

The author(s) declared that this work was conducted in the absence of any commercial or financial relationships that could be construed as a potential conflict of interest.

## Generative AI statement

The author(s) declared that generative AI was not used in the creation of this manuscript.

Any alternative text (alt text) provided alongside figures in this article has been generated by Frontiers with the support of

artificial intelligence and reasonable efforts have been made to ensure accuracy, including review by the authors wherever possible. If you identify any issues, please contact us.

## Publisher's note

All claims expressed in this article are solely those of the authors and do not necessarily represent those of their affiliated organizations, or those of the publisher, the editors and the reviewers. Any product that may be evaluated in this article, or claim that may be made by its manufacturer, is not guaranteed or endorsed by the publisher.

## References

- Adinet (2024). Adinet.Ahacentre.Org/Report. Available online at: <https://adinet.ahacentre.org/report/indonesia-flooding-in-ogan-ilir-south-sumatra-20240311> (Accessed May 10, 2024).
- Aryastana, P., Agung Yujana, C., Windy Candrayana, K., and Himawan Subiyanto, K. (2025). Analisis statistik kinerja dan koreksi kesalahan data curah hujan berbasis satelit di Provinsi Bali. *Majalah Geografi Indonesia*.
- BPS-Statistics Ogan Ilir regency (2025). *Ogan Ilir regency in figures 2025*, 16.
- Christian, C. (2022). "Application of the polder system in flood management in urban areas a case study," in *Proceedings of the 3rd Asia Pacific International Conference on Industrial Engineering and Operations Management, Johor Bahru, Malaysia*, September 13-15, 2022.
- Horváth, K., van Eschb, B., Vreeken, T., Piovesana, T., Talsmaa, J., and Pothofa, I. (2022). Potential of model predictive control of a polder water system including pumps, weirs and gates. *J. Process Control* 119, 128–140. doi:10.1016/j.jprocont.2022.10.003
- Hu, Y., Qin, T., Dong, G., Wang, L., Wang, M., Zhang, Q., et al. (2024). Flood modeling in a composite system consisting of river channels, flood storage areas, floodplain areas, polder areas, and flood-control-protected areas. *Water* 16, 825. doi:10.3390/w16060825
- Ignatius, S., Soeryantono, H., Anggraheni, E., and Sutjningsih, D. (2019). "Analysis of flood inundation in north sunter on the north sunter polder system performance," in *The 2<sup>nd</sup> international conference on green civil and environmental engineering. IOP Conf. Ser. Mater. Sci. Eng.* 669 (2019), 012039. doi:10.1088/1757-899X/669/1/012039
- Kalmah, F. X. S., and Schultz, B. (2015). *Evaluation of urban polder drainage system performance in jakarta case study kelapa gading area*.
- Latif, A. A., Pallu, M. S., Maricar, F., and Hatta, M. P. (2019). *Pengaruh tinggi bukaan pintu air terhadap bilangan froude dengan dasar tanah lempung pada saluran terbuka*. Prosiding Seminar Nasional Teknik Sipil.
- Mustamin, M. R., Maricar, F., and Hatta, M. P. (2021). Effects of nipa-nipa regulation pond on flood control of. *IOP Conf. Ser. Earth Environ. Sci.* 1134 (1), 012002. doi:10.1088/1755-1315/1134/1/012002
- NASA (2025). Gpm.Nasa.Gov. Available online at: <https://gpm.nasa.gov/data/directory> (Accessed Febuary 26, 2020).
- Noviadriana, D., Andawayanti, U., Juwono, P. T., and Dian, S. (2025). Indicators of index for polder services use partial least square and personal component analysis method. *ICWRDEP 2019 IOP Conf. Ser. Earth Environ. Sci.* 437 (2020), 012028. doi:10.1088/1755-1315/437/1/012028
- Reliefweb (2023). Reliefweb report. Available online at: <https://reliefweb.int/report/indonesia/indonesia-flooding-ogan-ilir-regency-south-sumatra-3-may-2023>.
- Researchgate (2010). Evaluation of urban polder drainage system performance in jakarta. Case study kelapa gading area. Available online at: <https://www.researchgate.net/publication/47844044> (Accessed Febuary 9, 2026).
- Salam, A. U., Tola, M., Selintung, M., and Maricar, F. (2014). On-line monitoring system of water leakage detection. *Arpn J. Eng. Appl. Sci.* 9 (10). October 2014.
- Satriani, S., Lopa, R. T., and Maricar, F. (2021). Storage capacity analysis of nipa nipa regulation pond using ripple method. *IOP Conf. Ser. Mater. Sci. Eng.* 1098 (2), 022054. doi:10.1088/1757-899X/1098/2/022054
- Stowa/MX Systems (2002). *DUFLOW reference manual*. The Netherland.
- Sumi, A. H., Suryadi, F. X., and Fachrurrozie, S. (2013). "Effects of uncontrolled landuse change to the inundation pattern and its possible measures," in *Case study: Lambidaro lowland subsystem in Palembang, 35th IAHR World Congress, Chengdu, China*, September 2013.
- Suryadi, F. X., Baedlowi, N., Ab Razak, M. S., Kalmah, (2014). "Hydraulic performance of urban polder water management and flood protection systems in jakarta," in *13th International Conference on Urban Drainage Sarawak, Malaysia*, September 2014, 7–12.
- Syarifudin, A. (2018). *Applied hydrology*. Bening's publisher.
- Syarifudin, A., Satyanaga, A., Wijaya, M., Moon, S.-W., and Kim, J. (2022). Sediment transport patterns of channels on tidal lowland. *Fluids* 7, 277. doi:10.3390/fluids7080277
- Volker, A. (1983). "Lesson from the history of impoldering in the world," in *Keynote paper in: final report polders of the world* (Lelystad, Netherlands: International Symposium).